

Supplement of:

Urban inland wintertime N₂O₅ and ClNO₂ influenced by snow-covered ground, air turbulence, and precipitation

5 Kathryn D. Kulju¹, Stephen M. McNamara¹, Qianjie Chen^{1†}, Jacinta Edebeli^{1,2}, Jose D. Fuentes³, Steven B. Bertman⁴, Kerri A. Pratt^{1,5*}

¹Department of Chemistry, University of Michigan, Ann Arbor, MI 48109, USA

²Paul Scherrer Institut, 5232 Villigen, Switzerland

10 ³Department of Meteorology and Atmospheric Science, Pennsylvania State University, University Park, Pennsylvania 16802, USA

⁴Institute of the Environment and Sustainability, Western Michigan University, Kalamazoo, Michigan 49008, USA

⁵Department of Earth and Environmental Sciences, University of Michigan, Ann Arbor, MI 48109, USA

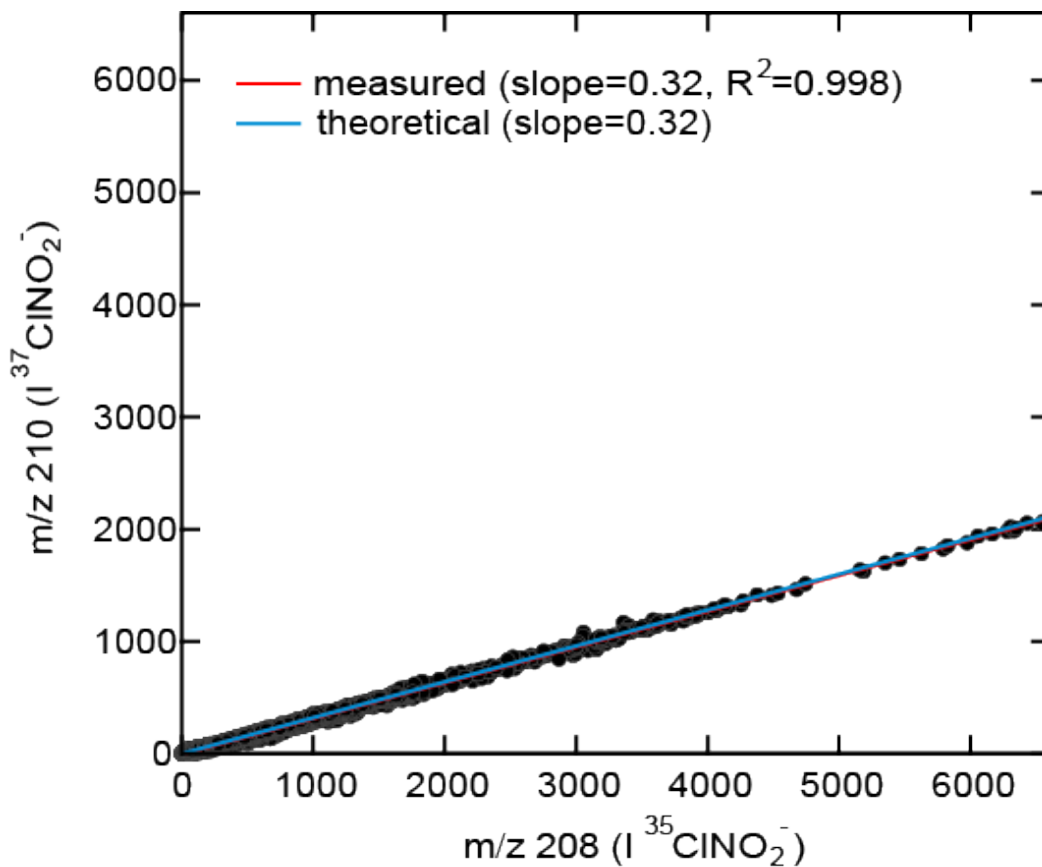
[†]Current: Department of Civil and Environmental Engineering, Hong Kong Polytechnic University, Hong Kong

Correspondence to: Kerri A. Pratt (prattka@umich.edu)

15

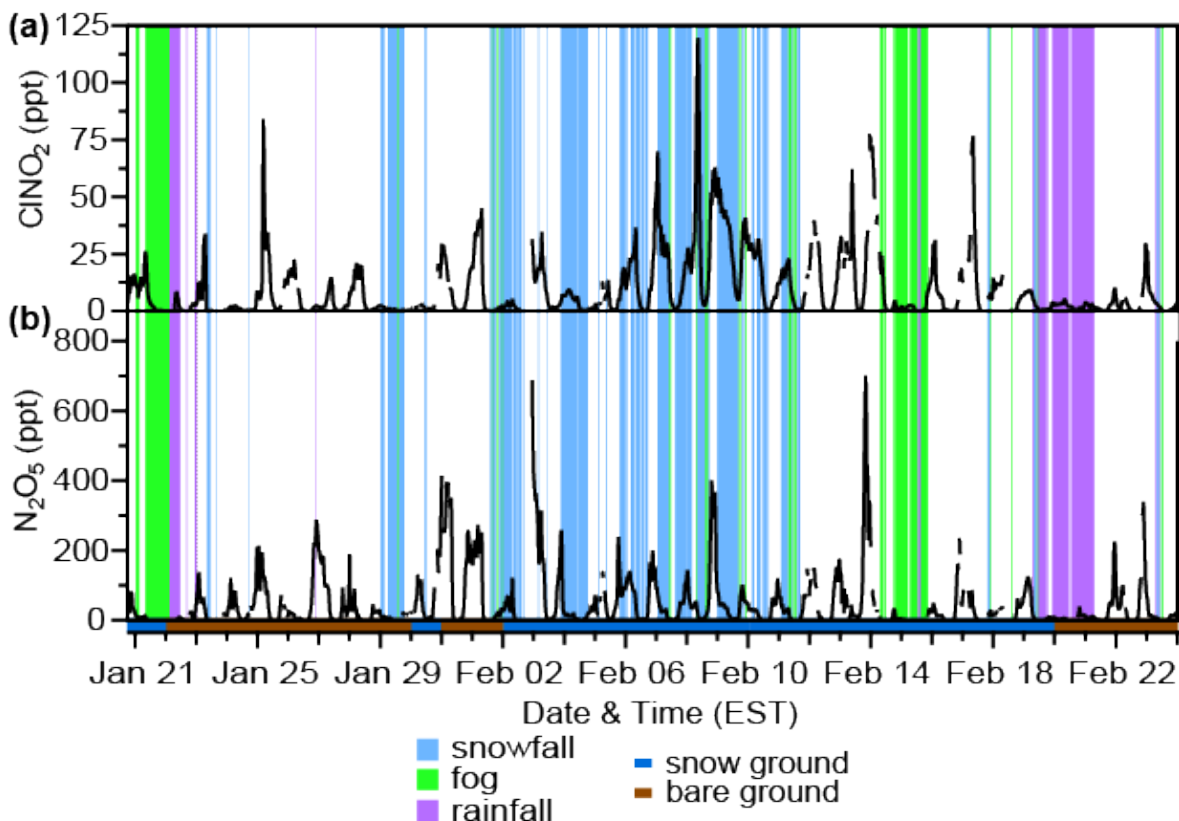
20

25



30

Figure S1: Plot of 5-min averaged, background subtracted, signals for $m/z\ 210$ vs. $m/z\ 208$, showing the isotopic ratio used to identify CINO_2 .



35 **Figure S2:** Mole ratios of 30 min averaged (a) ClNO_2 and (b) N_2O_5 during the campaign, and occurrence of snowfall (*light blue*), fog (*green*), and rainfall (*purple*). The shading below the x-axis represents ground cover – snow (*blue*) or bare ground (*brown*). Between 18:00 and 08:00 EST, where n=number of 30 min periods, the air was clear 72% of the time [n=726; 363 h], snowfall occurred 16% of the time [n=157; 78.5 h], rainfall occurred 6% of the time [n=63; 31.5 h], and fog occurred 6% of the time [n=58; 29 h]. The ground was snow-covered 57% of the study [20 d] and was bare for 43% of the study [15 d].

40

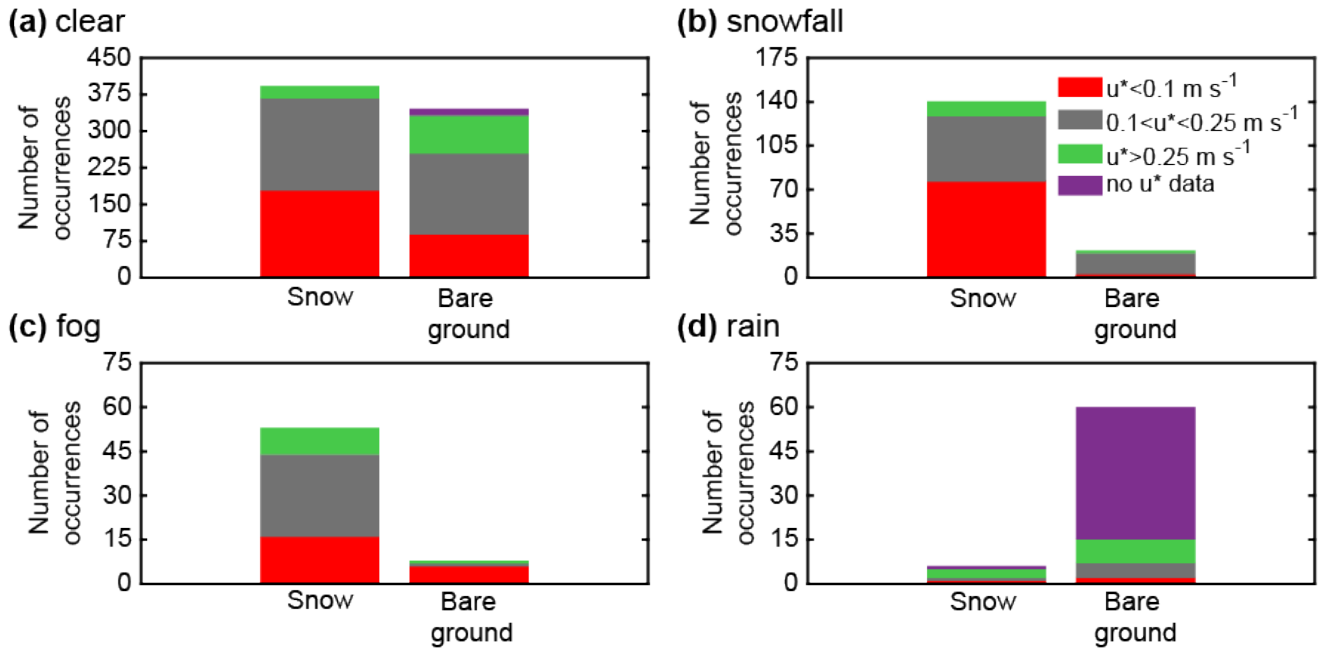
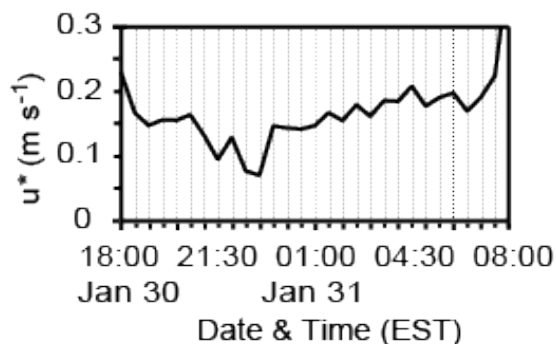
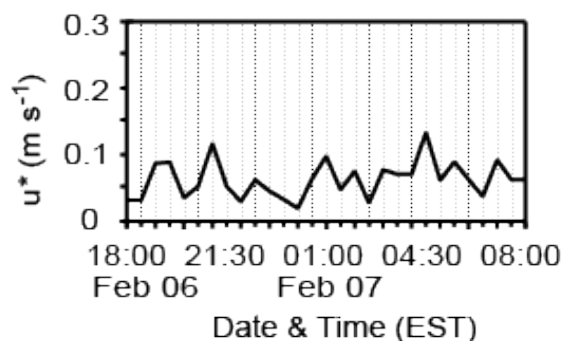


Figure S3: Stacked bar graphs showing the number of occurrences between 18:00 and 08:00 (30 min time resolution) of lower- ($u^* < 0.1 \text{ m s}^{-1}$), mid- ($0.1 < u^* < 0.25 \text{ m s}^{-1}$), and higher-turbulence ($u^* > 0.25 \text{ m s}^{-1}$) over snow-covered and bare ground, during (a) clear, (b) snowfall, (c) fog, and (d) rainfall conditions. Lower turbulence occurred 39% of the time, mid-turbulence occurred 42% of the time, and higher turbulence occurred 14% of the time. Snowfall and fog both primarily occurred over snow-covered ground (87% of the time). Rainfall occurred over bare ground 92% of the time. Clear conditions had snow-covered and bare ground 58% and 42% of the time, respectively. Lower-turbulence accompanied snow-covered ground 71% of the time, and higher-turbulence accompanied bare ground 64% of the time. The most frequent turbulence bin to occur during snowfall and fog was $u^* < 0.1 \text{ m s}^{-1}$, representing 59% and 55% of the occurrences during these periods, respectively. Clear conditions had $0.1 < u^* < 0.25 \text{ m s}^{-1}$ as the most frequent bin, followed by $u^* < 0.1 \text{ m s}^{-1}$, representing 48% and 36% of these periods, respectively. In contrast, the most frequent turbulence bin to occur during rainfall was $u^* > 0.25 \text{ m s}^{-1}$, representing 17% of all occurrences during rain and 55% of the periods for which measurements were available. Sonic anemometer measurements, and therefore calculated u^* values, are unavailable from February 20-21.

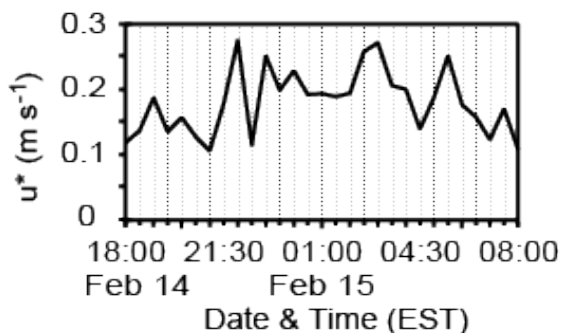
(a) clear



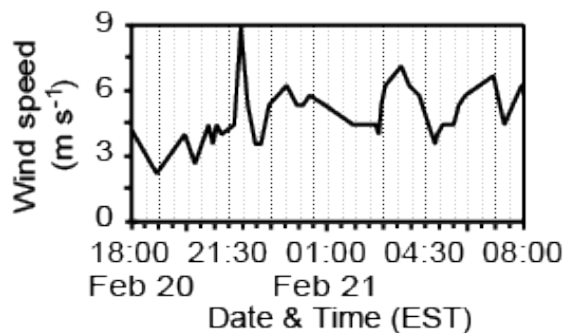
(b) snowfall



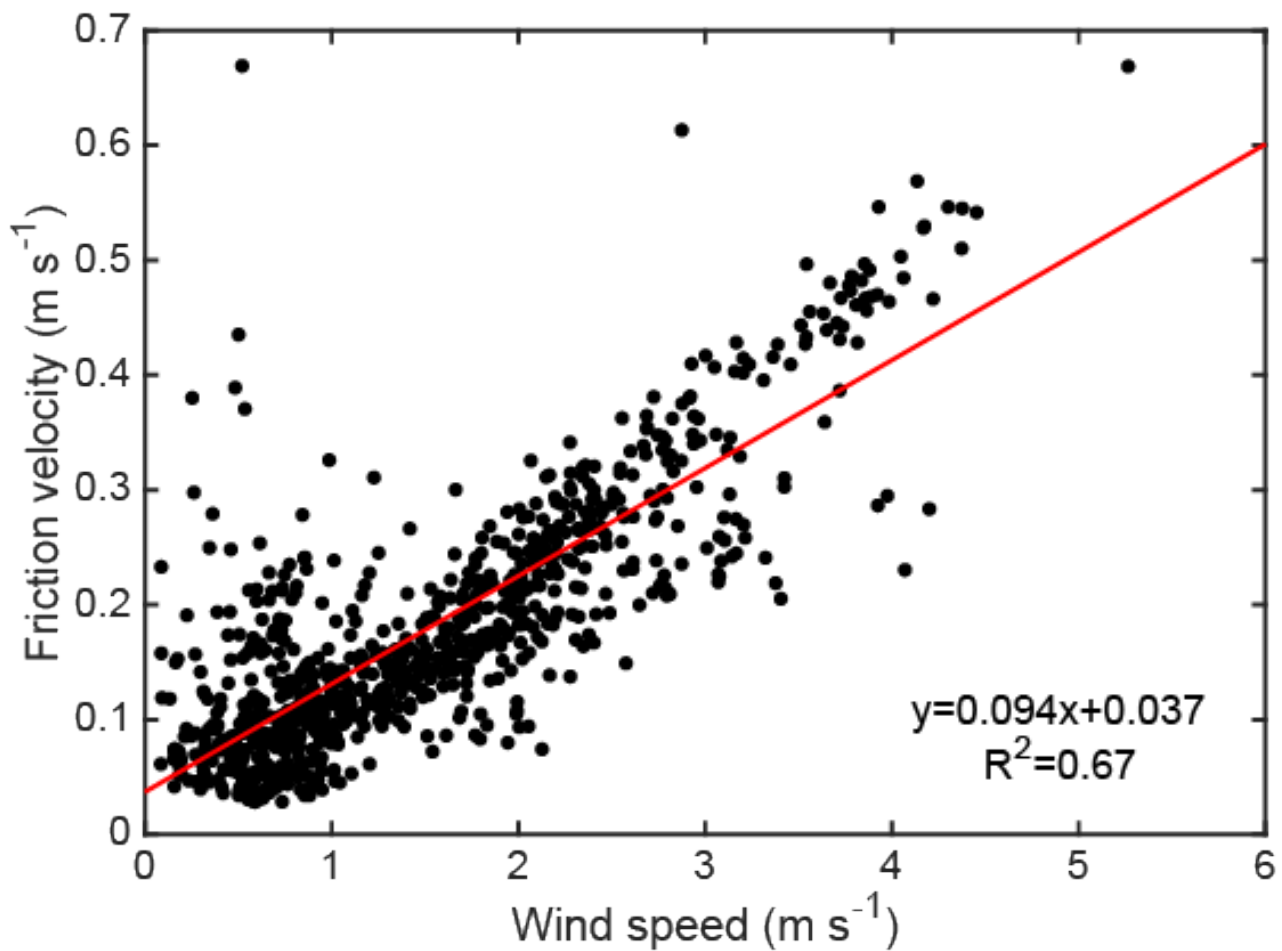
(c) fog



(d) rain



- 60 **Figure S4:** Friction velocity or wind speed between 18:00 and 08:00 EST for each of the case studies presented – (a) clear, (b) snowfall, (c) fog, and (d) rainfall. Friction velocity could not be calculated for the rainfall case because sonic anemometer data were unavailable. Wind speed is substituted, and the relationship between wind speed and friction velocity is described in Figure S5.



65

Figure S5: Relationship between friction velocity and wind speed, measured by the sonic anemometer at 20 Hz and plotted as 30 min averages. This linear regression indicates that for wind speed values greater than 2.3 m s⁻¹, the friction velocity was above 0.25 m s⁻¹ (consistent with higher turbulence in the context of this study).

70

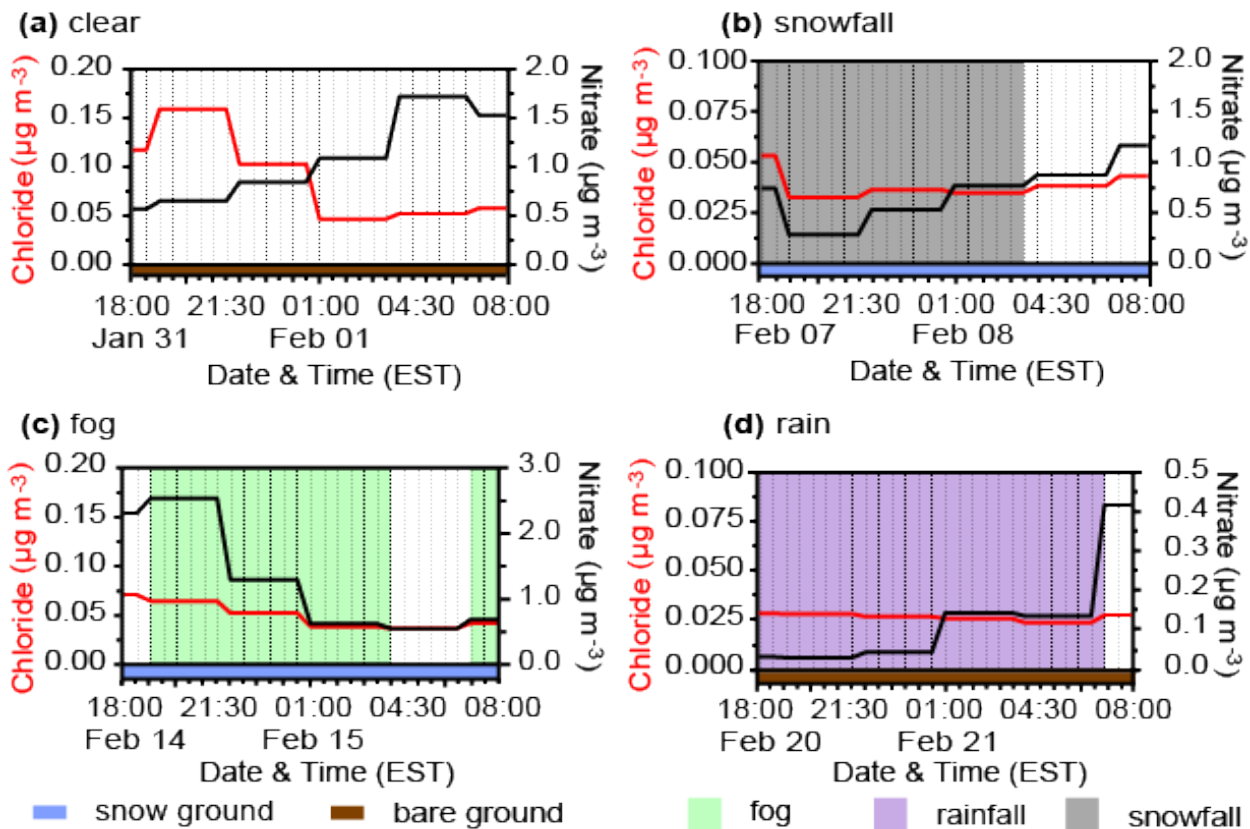
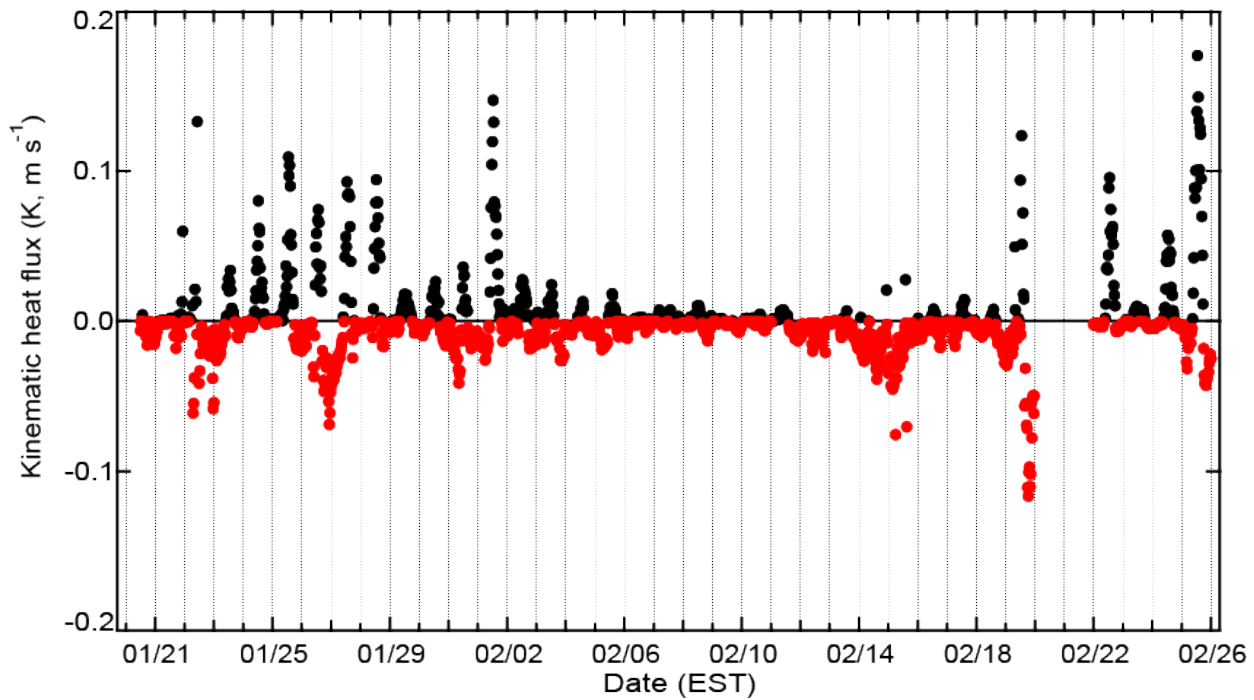


Figure S6: PM2.5 chloride and nitrate concentrations between 18:00 and 08:00 EST for each of the case studies presented – (a) clear air, (b) snowfall, (c) fog, and (d) rainfall. AIM-IC data were unavailable for the snowfall case night of February 06-07; therefore, we instead show a similar night, February 07-08 (the night after the snowfall case study) for comparison. The snowfall case study night and its substitution were similar in respect to snowfall and ground cover, but the substituted night had a higher friction velocity (average $u^*=0.12 \text{ m s}^{-1}$, whereas the snowfall case had an average $u^*=0.06 \text{ m s}^{-1}$).



80 **Figure S7:** Temporal variation of 30 min averaged kinematic heat flux throughout the duration of the study. Values less than zero, indicating a temperature inversion, are shown in red. A temperature inversion occurred during every night for which sonic anemometer data was available. Data was unavailable from Feb 20-21 due to complications associated with heavy rainfall.

85

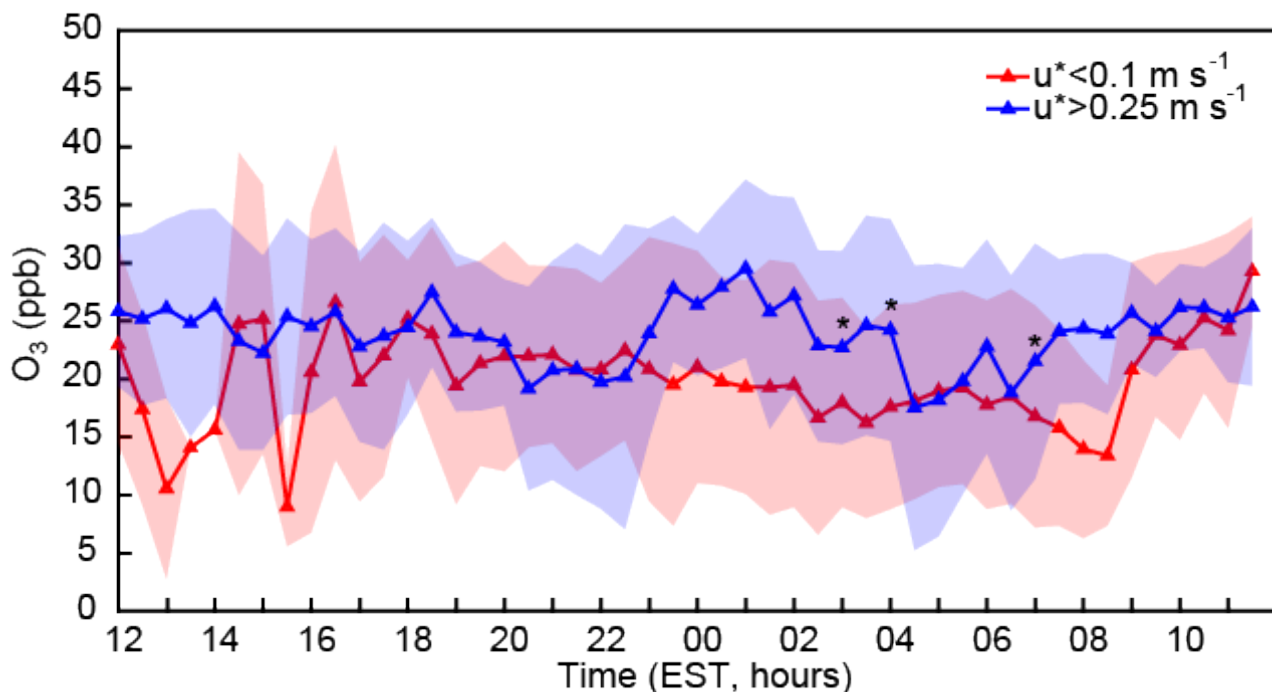


Figure S8: Diel patterns of 30 min averaged mole ratios of ozone binned by lower ($u^* < 0.1 \text{ m s}^{-1}$) and higher ($u^* > 0.25 \text{ m s}^{-1}$) turbulence conditions from January 20 - February 24. Shading represents one standard deviation. Asterisks represent statistically significant (t-test) differences at the $p < 0.05$ level between lower and higher turbulence conditions for each 30 min time period. Considering the statistically significantly different periods of 03:00, 04:30, and 07:00, ozone mole ratios are 7.0 ppb (1.4-fold) higher during higher-turbulence, conditions, on average. For the entire nighttime period (18:00-08:00), much of which is not statistically significantly different between the two turbulence bins, ozone mole ratios were 3.2 ppb (1.2-fold) higher during higher-turbulence conditions, on average.

95

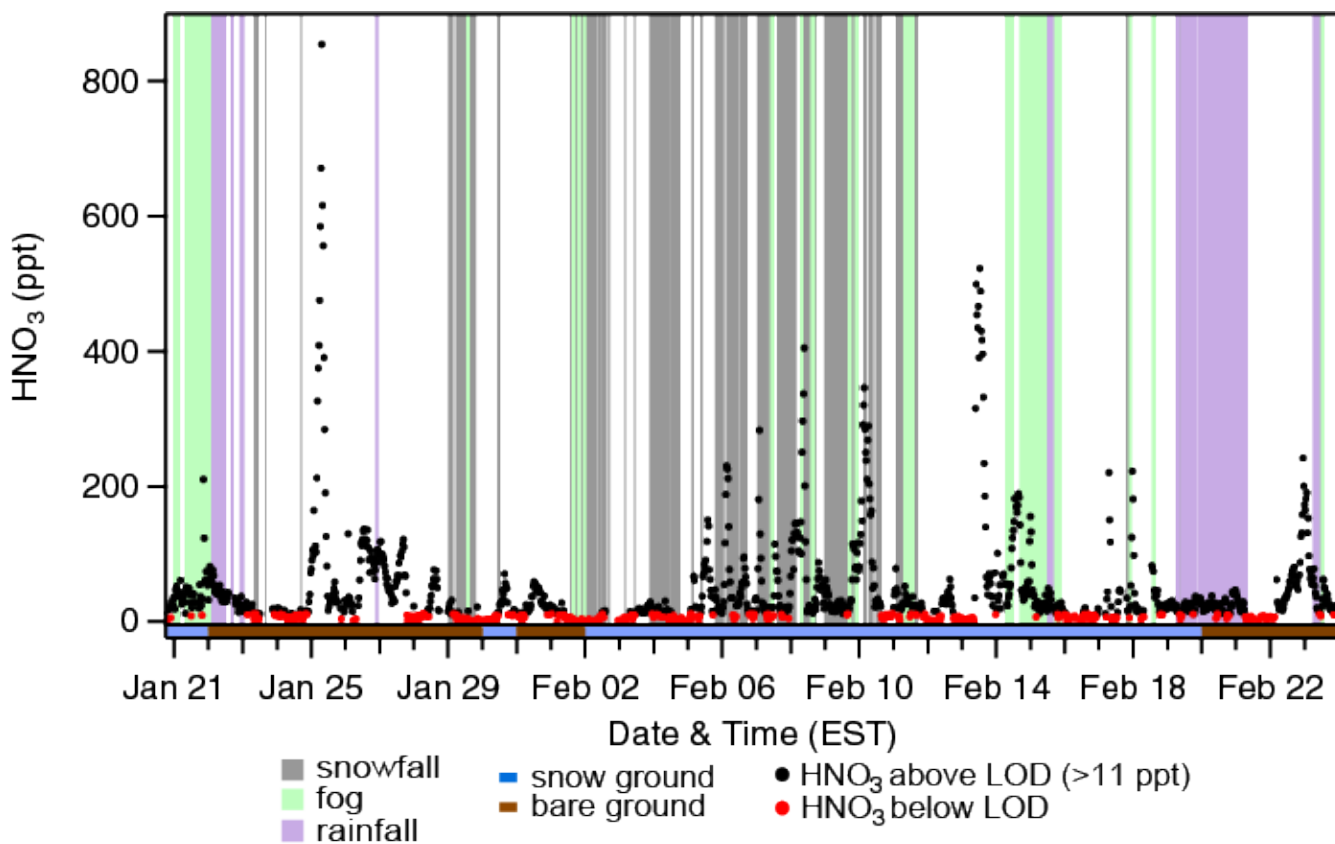


Figure S9: Mole ratios of 30 min averaged HNO₃ during the campaign, and occurrence of snowfall (gray), fog (green), and rainfall (purple). The shading below the x-axis represents ground cover – snow (blue) or bare ground (brown). Considering periods between 18:00 and 08:00 EST when HNO₃ was above LOD, where n=number of 30 min periods, the air was clear 63% of the time [n=376], snowfall occurred 18% of the time [n=105], rainfall occurred 10% of the time [n=60], and fog occurred 9% of the time [n=52]. The total number of 30 min periods for which HNO₃ was above LOD during nighttime was 593, or 60% of the nighttime data during the campaign. These data represent lower limits as they were not adjusted for the poor background scrubbing efficiency of 12±1%, and therefore, should only be viewed qualitatively.

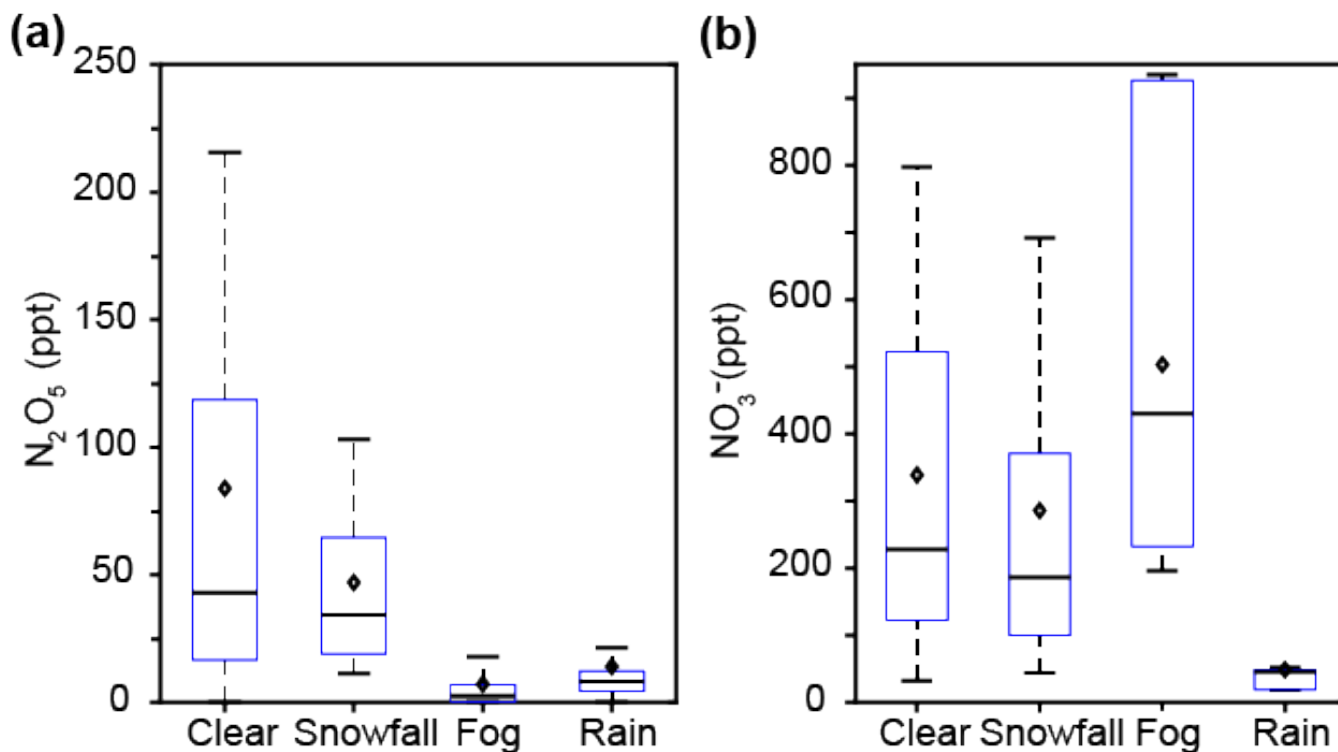
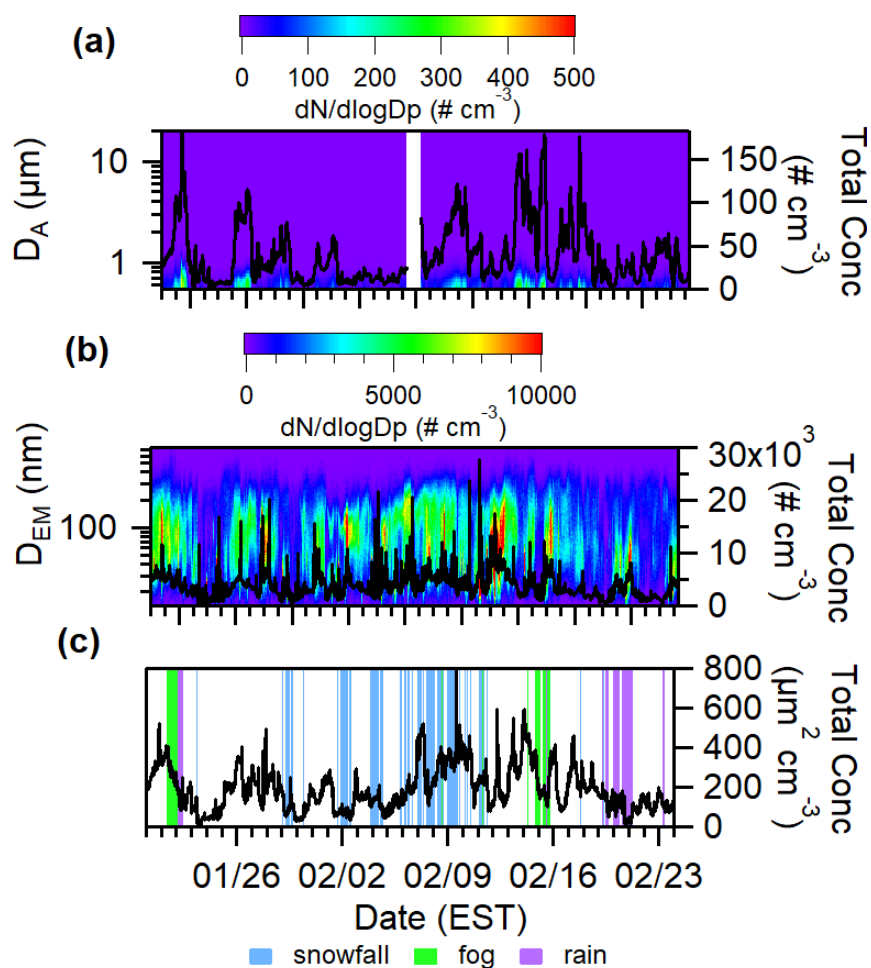


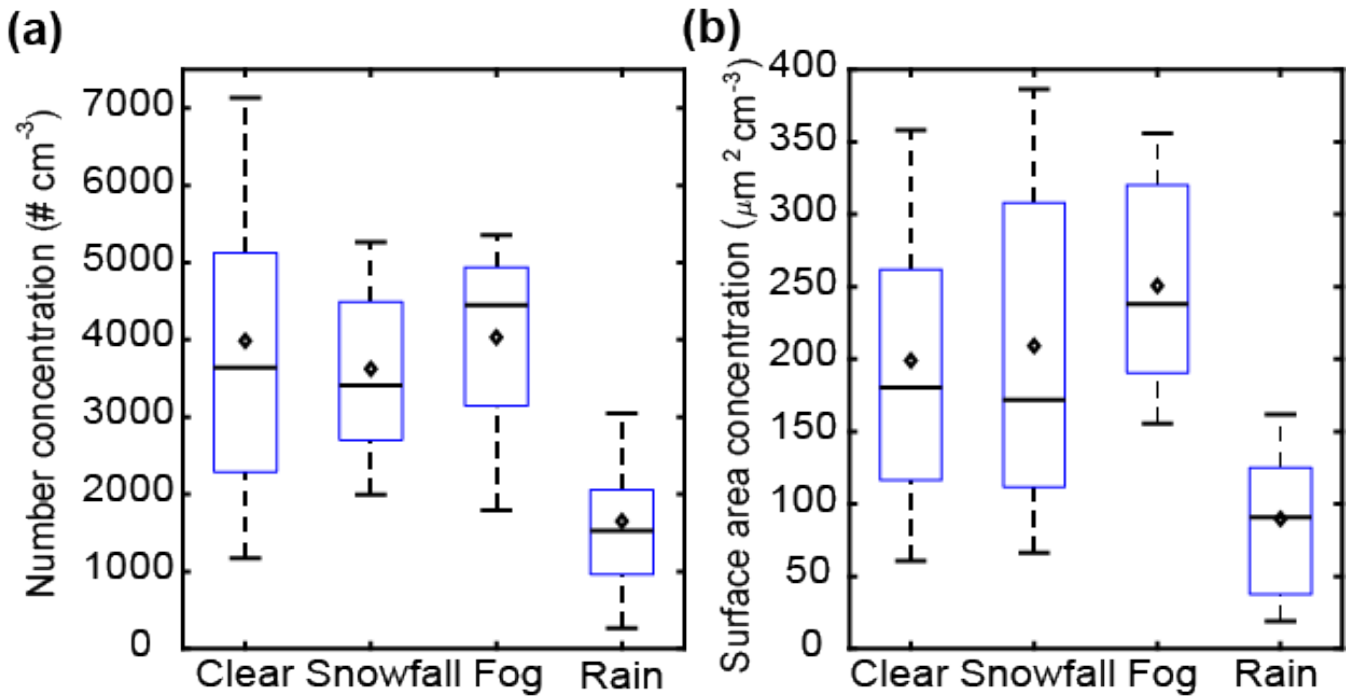
Figure S10: Box plots showing 30 min averaged mole ratios of (a) N_2O_5 and (b) $PM_{2.5} NO_3^-$ during clear conditions and weather events (snowfall, fog, and rain) from January 20-February 24. Bars represent the 10th, 50th, and 90th percentiles, boxes represent the 25th and 75th percentiles, and diamonds represent the means. Only nighttime data between 18:00 and 08:00 EST are included. The purpose of this figure is to show how the decrease in N_2O_5 compares to the increase in NO_3^- during fog in units that are appropriate for direct comparison. During fog, N_2O_5 mole ratios were lower by 77 ± 5 ppt, and $PM_{2.5} NO_3^-$ mole ratios were higher by 160 ± 20 ppt, in comparison to clear conditions.

110

115



120 **Figure S11:** Temporal variations in (a) aerosol size distributions and total number concentrations from the aerodynamic particle sizer (APS, model 3321, TSI, Inc.), which measured aerodynamic diameter (D_A) from 0.5-20 μm , (b) aerosol size distributions and total number concentrations from the scanning mobility particle sizer (SMPS, model 3082, TSI, Inc.), which measured electrical mobility diameter (D_{EM}) from 14.1-736.5 nm, and (c) total (D_{EM} 14.1-736.5 nm) surface area concentrations measured by the SMPS, where shading represents the occurrence of snowfall (light blue), fog (green), and rainfall (purple).



125

Figure S12: Box plots showing 30 min averaged submicron (D_{EM} 14.1-736.5 nm) (a) number and (b) surface area concentrations during nighttime (18:00 – 08:00 EST) clear conditions and weather events (snowfall, fog, and rain) from January 20-February 24. Bars represent the 10th, 50th, and 90th percentiles, boxes represent the 25th and 75th percentiles, and diamonds represent the means. Number concentrations are not statistically significantly different between clear and snowfall conditions ($p=0.06$), clear and fog conditions ($p=0.88$), or between snowfall and fog conditions ($p=0.06$). Surface area concentrations are not statistically significantly different between clear and snowfall conditions ($p=0.32$). The remaining comparisons between aerosol concentrations across the weather conditions are statistically significant ($p<0.05$). Number concentrations were 2300 ± 120 particles cm^{-3} (2.4 times) lower during rainfall in comparison to clear conditions. Surface area concentrations were 109 ± 6 $\mu\text{m}^2 \text{cm}^{-3}$ (2.2 times) lower during rainfall, and 52 ± 7 $\mu\text{m}^2 \text{cm}^{-3}$ (1.3 times) higher during fog, in comparison to clear conditions.

130

135

140

145

150 **Table S1:** Ranges, medians, averages, and 95% confidence intervals for mole ratios of ClNO₂ and N₂O₅, PM_{2.5} concentrations of Cl⁻ and NO₃⁻, temperature, relative humidity (RH), and friction velocity (u*) measured across the entire campaign, between 18:00-08:00 EST. Data below the limit of detection (LOD) were applied as $\frac{1}{2} \times \text{LOD}$ in calculations.

	Clear	Snowfall	Fog	Rain
ClNO₂ range (ppt)	0.05-84	0.05-70	0.05-76	0.05-5.25
ClNO₂ median (ppt)	6.3	11.9	1.0	2.59
ClNO₂ average ± 95% confidence interval (ppt)	11.8±0.7	16.8±0.7	5.0±0.6	2.27±0.06
N₂O₅ range (ppt)	0.15-702	0.15-257	0.15-55	0.15-289
N₂O₅ median (ppt)	43	34	2.4	8
N₂O₅ average ± 95% confidence interval (ppt)	84±5	47±2	7.1±0.6	14±2
Cl⁻ range (µg m⁻³)	0.040-0.910	0.040-0.645	0.197-0.717	0.03-0.57
Cl⁻ median (µg m⁻³)	0.228	0.213	0.374	0.12
Cl⁻ average ± 95% confidence interval (µg m⁻³)	0.257±0.007	0.258±0.006	0.456±0.008	0.22±0.01
NO₃⁻ range (µg m⁻³)	0.03-3.9	0.07-2.50	0.11-3.9	0.027-0.707
NO₃⁻ median (µg m⁻³)	0.64	0.53	1.17	0.118
NO₃⁻ average ± 95% confidence interval (µg m⁻³)	0.95±0.04	0.81±0.03	1.38±0.04	0.126±0.007
Temperature range (K)	258.5-288.7	260.3-271.9	260.6-282.8	273.2-288.8
Temperature median (K)	271.2	264.9	277.3	283.3
Temperature average ± 95% confidence interval (K)	270.8±0.3	265.8±0.2	276.7±0.2	282.1±0.2
RH range (%)	39-97	64-97	73-100	39-97
RH median (%)	76.0	84.0	96.0	92.5
RH average ± 95% confidence interval (%)	75.0±0.5	82.9±0.3	93.7±0.3	90.2±0.4
u* range (m s⁻¹)	0.032-0.498	0.027-0.509	0.029-0.719	0.03-0.74
u* median (m s⁻¹)	0.133	0.102	0.123	0.30
u* average ± 95% confidence interval (m s⁻¹)	0.150±0.004	0.129±0.004	0.162±0.007	0.36±0.01

155 **Table S2:** Ranges, medians, averages, and 95% confidence intervals for mole ratios of ClNO₂ and N₂O₅, PM_{2.5} concentrations of Cl⁻ and NO₃⁻, temperature, relative humidity (RH), and friction velocity (u*) observed during each of the case study periods, between 18:00-08:00 EST. Data below the limit of detection (LOD) were applied as $\frac{1}{2} \times \text{LOD}$ in calculations.

	Clear (Jan 31- Feb 01)	Snowfall (Feb 06-07)	Fog (Feb 14-15)	Rain (Feb 20- 21)
ClNO₂ range (ppt)	1.5-45	2.4-70	0.6-4.5	0.6-3.7
ClNO₂ median (ppt)	21	28	1.6	1.8
ClNO₂ average ± 95% confidence interval (ppt)	23±5	30±6	1.8±0.4	2.0±0.3
N₂O₅ range (ppt)	75-274	22-201	1.1-31	7.1-40
N₂O₅ median (ppt)	207	71	2.7	11
N₂O₅ average ± 95% confidence interval (ppt)	200±16	82±21	5±3	13±4
Cl⁻ range (µg m⁻³)	0.05-0.16	0.033-0.043*	0.037-0.065	0.023-0.028
Cl⁻ median (µg m⁻³)	0.08	0.036*	0.042	0.026
Cl⁻ average ± 95% confidence interval (µg m⁻³)	0.09±0.04	0.037±0.004*	0.047±0.04	0.026±0.03
NO₃⁻ range (µg m⁻³)	0.7-1.7	0.3-1.2*	0.5-2.5	0.025-0.4
NO₃⁻ median (µg m⁻³)	1.1	0.7*	0.7	0.1
NO₃⁻ average ± 95% confidence interval (µg m⁻³)	1.2±0.4	0.7±0.3*	1.1±0.7	0.2±0.1
Temperature range (K)	273.1-276.6	263.7-266.1	276.0-282.8	273.2-287.6 [†]
Temperature median (K)	274.6	265.0	280.1	278.2 [†]
Temperature average ± 95% confidence interval (K)	274.8±0.4	265.1±0.3	279.7±0.9	279±2 [†]
RH range (%)	62-76	63-88	92-100	85-93
RH median (%)	72	79	96	89
RH average ± 95% confidence interval (%)	72±1	78±3	96±1	89±1
u* range (m s⁻¹)	0.07-0.23	0.02-0.13	0.11-0.28	2.2-8.9 (0.25-0.46) [†]
u* median (m s⁻¹)	0.16	0.06	0.19	4.5 (0.46) [†]
u* average ± 95% confidence interval (m s⁻¹)	0.16±0.01	0.06±0.01	0.18±0.02	5.0±0.5 (0.50±0.08) [†]

160 *Because the AIM-IC was not operational during the snowfall case study, the following night (February 07-08) is substituted for concentrations of Cl⁻ and NO₃⁻. The snowfall case study night and its substitution were similar in respect to snowfall and ground cover, but the substituted night had a higher friction velocity (average u*=0.12 m s⁻¹, whereas the snowfall case had an average u*=0.06 m s⁻¹).

165 † Because the sonic anemometer was not operational during the rainfall case, we use temperature and wind speed values from the Kalamazoo–Battle Creek International Airport (KAZO) located ~7 km to the southeast and retrieved from Weather Underground (<https://www.wunderground.com/history/daily/us/mi/kalamazoo/KAZO>). We provide estimated u^* values in parentheses, calculated using the linear regression of u^* vs wind speed in Figure S5.